XV International Conference on Durability of Building Materials and Components
DBMC 2020, Barcelona
C. Serrat, J.R. Casas and V. Gibert (Eds)

Monitoring Durability of Limestone Cement Paste Stored at Conditions Promoting Thaumasite Formation

Konstantinos Sotiriadis[1], Michal Hlobil[1], Jaromír Toušek[2], Dita Machová[1], Petra Mácová[1], Michal Vopálenský[1] and Alberto Viani[1]

[1] Institute of Theoretical and Applied Mechanics of the Czech Academy of Sciences, Prosecká 809/76, 19000 Prague 9, Czechia, sotiriadis@itam.cas.cz

[2] CEITEC – Central European Institute of Technology, Masaryk University, Kamenice 5/A4, 62500 Brno, Czechia, tousek@chemi.muni.cz

Keywords: *Limestone Cement, Thaumasite Sulfate Attack, Microstructure, Solid State NMR Spectroscopy, X-Ray Micro-Computed Tomography.*

1 Introduction

Portland-limestone cements, developed as alternative to ordinary Portland cement, are characterized by competitive properties and lower environmental impact, however, they are susceptible to the thaumasite sulfate attack (TSA). A model predicting the mechanical properties of cementitious materials exposed to conditions facilitating TSA would allow for optimizing concrete formulation in terms of durability and environmental impact. To this aim, this study is focused on obtaining necessary data about microstructure and strength.

2 Experimental

Portland-limestone cement paste (water-to-cement ratio of 0.45) cylinders (d=20 mm; h=50 mm) were produced with a commercial CEM II/B-LL cement, and immersed in $MgSO_4$ solution (S) (20 g/L SO_4^{2-} content), and water (W) as reference, at 5 °C. The number of specimens used in each test for each exposure environment and storage period are shown below in brackets. Pore structure and deterioration characteristics were assessed with X-ray micro-computed tomography (1). Structural parameters (porosity, ϕ; specific surface area of pores, S_v; mean curvature of pores, M_v) were extracted by analyzing appropriate volumes of interest. Structural characteristics were correlated with compressive strength (5). Phase changes were investigated with X-ray powder diffraction and ^{29}Si MAS NMR spectroscopy (1 for W and 8 for S).

3 Results

Sulfate attack evolved through the formation of concentric crack patterns, followed by expansion and detachment of the damaged part of the specimen that was in direct contact with the corrosive solution. The average values of structural parameters, derived from quantitative image analysis of tomographic images, indicated a similar microstructure for the sound part of the specimens exposed to W (ϕ = 0.53%, S_v = 0.91 mm^{-1}, M_v = 227.39 mm^{-2}) and S (ϕ = 0.65%, S_v = 1.75 mm^{-1}, M_v = 373.37 mm^{-2}) solutions. This suggested a front-like deterioration, moving from the surface towards the center of the specimen, and resulting in rapid decline of structural integrity and relative compressive strength (76% decrease at 3.5 months).

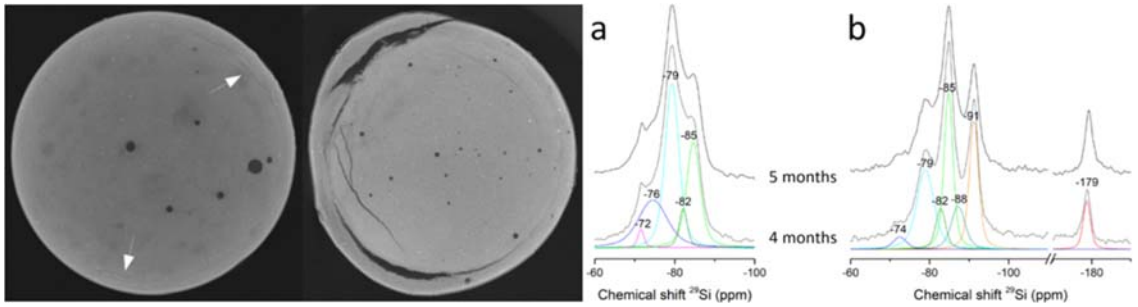

Figure 1. Left: Cross sectional XmCT images of specimens exposed to magnesium sulfate solution for 3 months (left) and 4 months (right); white arrows indicate cracks formed due to sulfate attack. – Right: ^{29}Si MAS NMR spectra collected at 4 and 5 months for specimens stored in water (a) and for samples obtained from the deteriorated surface of specimens exposed to magnesium sulfate solution (b). Black curves: experimental spectra; Colored curves: deconvoluted spectra (─72 ppm: Q^0; ─74, ─76 and ─79 ppm: Q^1; ─82 ppm: Q^1(1Al); ─85 ppm: Q^2; ─88 ppm: Q^2_u; ─91 ppm: Q^3(1Al); ─179 ppm: SiO_6).

X-ray powder diffraction data indicated the participation of limestone in cement hydration (decrease in calcite content ─ formation of carboaluminate hydrates). During sulfate attack, thaumasite, ettringite and gypsum formed at the expense of portlandite, calcite and monocarboaluminate hydrate; reduced amorphous content with time evidenced C─S─H deterioration. One-pulse ^{29}Si MAS NMR spectra indicated that sulfate attack promoted the polymerization of the silicate chains in C─S─H phase and led to the formation of condensed aluminosilicate structures, as a consequence of C─S─H deterioration.

ORCID

Konstantinos Sotiriadis: http://orcid.org/0000-0002-9848-4028
Michal Hlobil: http://orcid.org/0000-0001-5818-7320
Jaromír Toušek: http://orcid.org/0000-0002-3231-2370
Dita Machová: http://orcid.org/0000-0001-9956-7282
Petra Mácová: http://orcid.org/0000-0002-8277-133X
Michal Vopálenský: http://orcid.org/0000-0002-9932-6486
Alberto Viani: http://orcid.org/0000-0002-6019-1094

References

Andersen, M.D., Jakobsen, H.J. and Skibsted, J. (2004). Characterization of white Portland cement hydration and the C-S-H structure in the presence of sodium aluminate by ^{27}Al and ^{29}Si MAS NMR spectroscopy *Cement and Concrete Research*, *34*(5), 857–868. doi: 10.1016/j.cemconres.2003.10.009

Grimmer, A.R., von Lampe, F. and Mägi, M. (1986). Solid-state high-resolution ^{29}Si MAS NMR of silicates with sixfold coordinated silicon *Chemical Physics Letters*, *132*(6), 549–553. doi: 10.1016/0009-2614(86)87122-6

L' Hôpital, E., Lothenbach, B., Le Saout, G. and Kulik, D. (2015). Incorporation of aluminium in calcium-silicate-hydrates *Cement and Concrete Research*, *75*, 91–103. doi: doi:10.1016/j.cemconres.2015.04.007

Rawal, A., Smith, B.J., Athens, G.L., Edwards, C.L., Roberts, L., Gupta, V. and Chmelka, B.F. (2010). Molecular silicate and aluminate species in anhydrous and hydrated cements *Journal of the American Chemical Society*, *132*(21), 7321–7337. doi: 10.1021/ja908146m

Richardson, I.G., Skibsted, J., Black, L. and Kirkpatrick, R.J. (2010). Characterization of cement hydrate phases by TEM, NMR and Raman spectroscopy *Advances in Cement Research*, *22*(4), 233–248. doi: 10.1680/adcr.2010.22.4.233

Walkley, B. and Provis, J.L. (2009). Solid-state nuclear magnetic resonance spectroscopy pf cements *Materials Today Advances*, *1*, 100007. doi: 10.1016/j.mtadv.2019.100007